SSRG International Journal of Electrical and Electronics Engineering
ISSN: 2348 – 8379 /doi:10.14445/23488379/IJEEE-V7I12P101

Volume 7 Issue 12, 1-9, December 2020

Application of I.R. Calorimetric Method for Power Losses Measurements in Power Electronics Components and Systems

Elysée Obame Ndong[#1], Olivier Gallot - Lavallée[*2], Frédéric Aitken[#3]

[1#]*Département Génie Electrique, Ecole Polytechnique de Masuku, Université des Sciences et Techniques de Masuku & STM, M2elab, Franceville; Gabon*

[2#] *Univerté Grenoble Alpes, CNRS, Grenoble-INP, G2Elab, F-38000 Grenoble, France*

Abstract *— Calorimetric measurement methods allowed to investigate power losses for high frequency and high-efficiency power electronics components and systems, where electrical methods reach their limits. In the present work, a special calorimetric method based on radiation heat transfer between the device under test and the measuring cell is used for power loss measurements of electrical resistance, a fly-back converter, a self-inductance, and a film capacitor for illustration. The aim is to highlight our device's experimental performance, for which the accuracy is close to 2% for a measurable power loss higher than 100 mW.*

Keywords — *Calorimeter, dielectric loss, heat radiation, measurement, power loss.*

I. INTRODUCTION

Power electronics components are used in a wide range of applications [1]. These components are subjected to significant thermal stresses in operating conditions due to heat losses by conduction and switching. Other specific phenomena such as hysteresis in ferromagnetic materials, dielectric polarization, and partial discharges can cause these losses. The thermal gradients exposed to repetitive thermo-mechanical stresses affect electrical components' lifetime characteristics [2]. Regarding standards requirements to ensure reliable operation conditions and safety, accurate estimates of power losses have become substantial for proper thermal management [3]. Recent advances toward integration and higher operating frequencies in power electronics systems have even increased the design process's important to assess system performance and optimize design characteristics [4].

Power loss estimates by analytical and numerical modeling are particularly interesting. However, the model's validation often requires comparisons with accurate experimental measurements, mostly when the loss mechanisms are nonlinear.

Evaluation of low power loss is a challenge with high-efficiency electrical components and high frequency [5, 6].

Two sorts of power loss measurement techniques exist the electrical and calorimetric measurement methods. The interest in electrical methods is well known. However, these methods are no longer suitable for high-frequency signals and highly distorted signals, such as pulse width modulation in which high variations of current and voltage are encountered.

The calorimetric principle is considered the most promising method for accurate power loss measurements [7–14]. This method has the advantage of measuring power losses under normal operating conditions, and it is also independent of electrical quantities supplying the device under test (DUT). Disadvantages are that the measurement is usually performed in steady-state, and therefore it is time-consuming.

Different calorimetric methods are known today, which are either based on adiabatic [5, 7, 15, 16], isoperibolic or quasi-adiabatic [17–23], isothermal [24, 25], or heat flow [26] principles have been widely used in power electronics to measure power losses of magnetic components, capacitors, switching semiconductors, superconductors, power converters and electrical machines [4]. Most of these methods show remarkable accuracies, as seen in TABLE I giving the main ones.

However, it can be seen (TABLE I) that these calorimeters still present some limitations in measurable power loss range, frequency, temperature, applied voltage, or the tested component geometry as highlighted in [27]. Particularly measurements of a few tens of milliwatts to several watts in a relatively wide range of temperature remain challenging.

To improve some of the disadvantages observed in recent calorimeters for specific research applications, mostly the temperature range, we designed from analytical modeling [28] and implemented an original thermal radiation calorimeter. Our calorimeter's originality is based on the fact that heat transfer between a measuring cell and a DUT is achieved by radiation.

The radiation calorimeter has been designed for operating Temperatures ranging from –50 °C to 150 °C with applied voltage up to 3 kV rms and frequency up to 1 MHz. The characterization of power loss is achieved regardless of the DUT geometry with a minimum measurable heat power

loss of 15 mW. These features and the temperature and the frequency ranges are defined to investigate heat loss in the power converter and dielectric materials. More details about the calorimeter and its theoretical performance have already been described [27–29].

In the present work, we propose using our calorimetric method to measure power losses with an electrical resistor, a fly-back converter, a self-inductance for loss separation, and a film capacitor. The aim here is to illustrate the experimental behavior and the global accuracy of our I. R. calorimetric method devoted to low loss measurements with these simple cases.

TABLE 1. Main characteristics of current calorimeters applied in electrical engineering measurements, R.T. stands for Room Temperature

Type of calorimeter		Measurements range			
		Temperature (°C)	Frequency (Hz)	Loss (W)	Accuracy
adiabatic	[5]	20 to 70	-	0.2 to 1	> 10% (2)
	[6]	RT to 80	0 to 1.3 M	0.8 to 30	2%
	[11]	0 to 90	-	10 to 90	3%
	[13]	RT	-	74 to 200	< 1%
	[14]	-	-	1 to 30	> 9%
	[15]	20 to 80	-	10 to 100	< 4%
	[16]	RT to 80	-	1 to 50	5.9%(1)
Isoperibolic	[17]	RT	-	1 to 1 k	0.7%
	[19]	RT	-	up to 1 k	2%
	[20]	RT	-	1 to 13 k	5%
	[21]	RT	100 k	~ 0.4	> 10%
	[22]	RT	-	2.68	5%
	[23]	RT	~ 200 k	20 to 40	15%
Isothermal	[24] [25]	-50 to 100	10^3 to 10^6	10^{-2} to 10	1.5%
Heat flow	[26]	RT	-	< 50	18%(3)

(1) at T=30 °C and P= 1W, (2) at 0.4 W, (3) at T=50 °C and P= 1W. k = 1000.

II. CALORIMETRIC DEVICE

The radiation calorimeter has been designed and implemented to characterize power losses in materials and devices under electrical constraints (Fig 1). In this calorimeter, heat power losses between the DUT and the isothermal calorimetric block (measuring cell) are achieved by infrared radiation.

The measuring cell is shown in Fig. 2, and it is made in two half copper spheres with an external diameter of 200 mm and 10 mm thickness. These dimensions were largely influenced by the calorimeter developed in [24]. The copper used here is the Oxygen Free High Conductivity type (OFHC) with 392.3 W/(m K) thermal conductivity and 389.4 J/(kg K) specific heat capacity at 300 K. [30]. The measuring cell's geometry, thickness, and manufacturing material are selected to achieve an isothermal body. This is why the contact section between the half spheres has also been optimized.

The half-spheres are assembled by a system of eight screw–nuts to minimize the thermal contact resistance between them. Their external surface has been polished and golden (Fig. 2) to lower their thermal emissivity. This favors the cell's temperature homogenization since heat transfer by radiation is lowered outside, and the gilding ensures the cell's protection against oxidation.

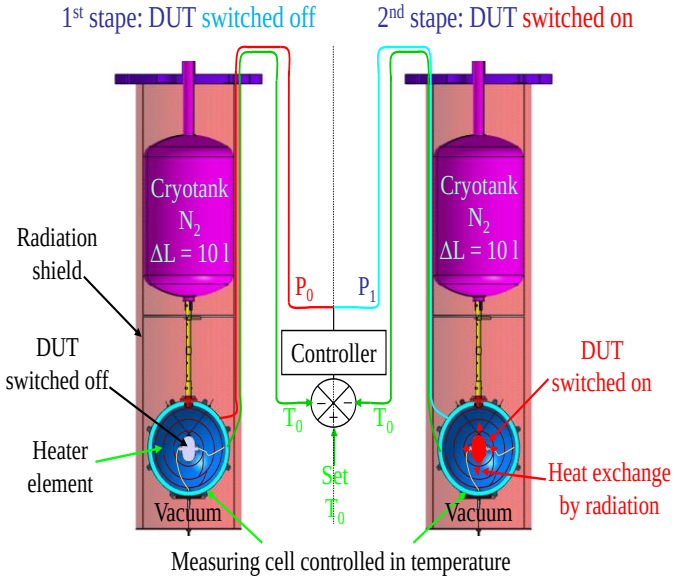

Fig. 1. Overview of our new calorimetric setup and representation of its measurement principle (differential method). The calorimeter is equipped with a liquid nitrogen tank that loses about 0.4 l/h (= 18 W) of liquid nitrogen by evaporation when the measuring cell is controlled at 30 °C with 21 °C ambient temperature. Heat power required by the controller to set 30 °C on the measuring cell is about 3 W. Measurements are performed in the calorimetric enclosure exhausted at 10^{-6} mbar. The enclosure time of the enclosure to reach the indicated pressure is about 12 h. The stabilization of the calorimetric system's temperature (steady-state thermal regime) is about 48 h, after which measurements can start.

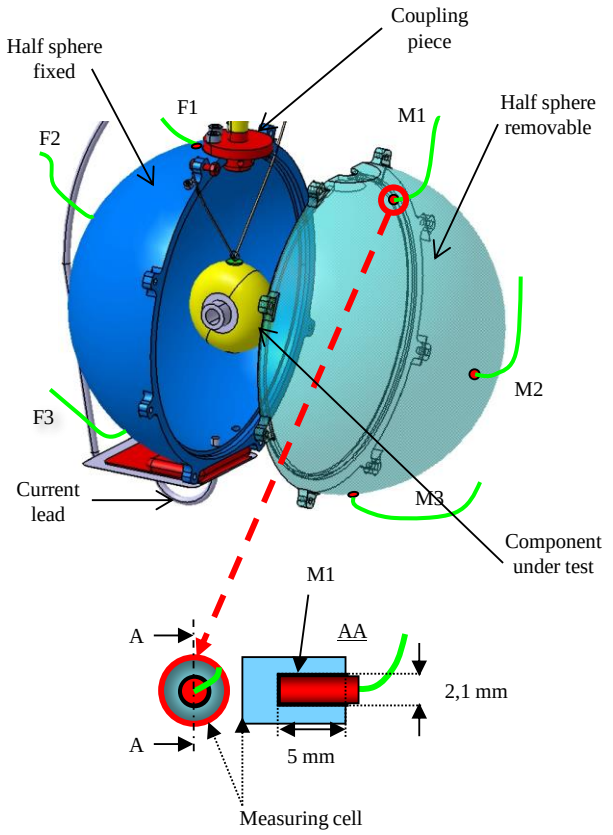

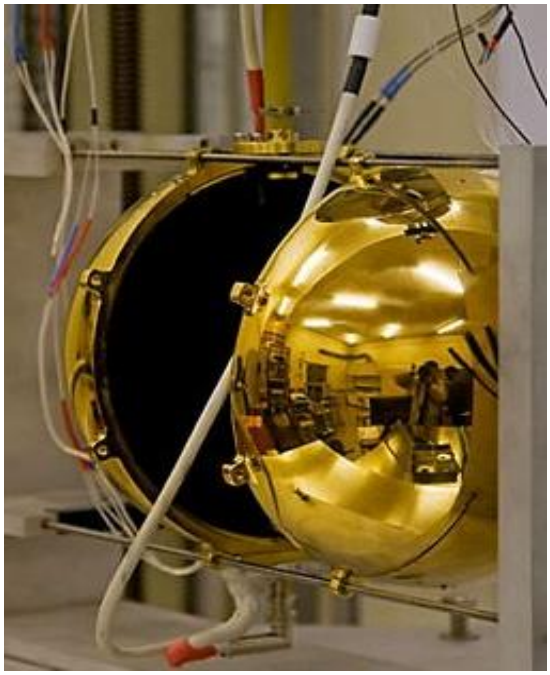

Fig. 2. Constitution of the measuring cell. The external surface is polished and golden, while the internal surface is rough and coated with Nextel – velvet coating 811 – 21® black paint. Six cylindrical Pt100 sensors (F1, F2, F3, M1 M2, and M3) are introduced in holes drilled in the measuring cell thickness and glued.

However, the internal surfaces are rough and coated by Nextel® Velvet Coating 811–21 black paint having 0.97 normal emissivities. The latter is temperature independent [31], and it is almost stable when the wavelength ranges from 0 µm to 15 µm [32]. The aim here is to approach the black body characteristics.

Cylindrical Pt100 probes control the measuring cell temperature. To assess the measuring cell's thermal homogeneity, three sensors noted F1, F2 and F3 are located on the fixed half-sphere (Fig. 2) and three others M1, M2, and M3 removable half sphere. However, temperature management is carried out only by one of these sensors (F2). The tolerance class of our sensors is 1/3 DIN B, according to EN 60 751 standards with a resolution of 0.001 °C [33]. These probes' characteristics and the measuring cell pre-test characterizations are highlighted in [27–29].

The calorimeter allows thus to handle the DUT in an isothermal controlled environment. The device's accuracy is better than 2% when a dissipated heat power measured is higher than 100 mW [27]. The maximum heat power loss measurable is about 10 W when the measuring cell temperature set point is 100 °C (table 2), and the measurement time does not exceed 180 min.

During measurements, heat power dissipated by the DUT is deducted from a differential method. In steady-state thermal condition, one measures the heat power P0 supplied by the temperature controller to the measuring cell when switched off (DUT off). One measures the heat power P_1 supplied by the controller when the tested component is energized (DUT on). The power losses dissipated by the sample noted P is given by (1)

$$\mathbf{P = P_0 - P_1 + \Delta P} \quad \textbf{(1)}$$

The quantity ΔP stands for the physical measurement error due to current leads and the variation of the heat power exchanged by the measuring cell with surrounding objects. The influence of ambient temperature is seen negligible [28] (almost stable external temperature). Therefore heat power exchanged between the measuring cell and surrounding objects is mainly influenced by the status change of the DUT (i.e., DUT off and DUT on) when P_0 and P_1 are measured and by the change of the cryotank temperature. Finally, it should be noted that the Temperature of the DUT is necessarily higher than that of the measuring cell (DUT on) and is not measurable in the calorimeter. However, the temperature difference between the measuring cell and the DUT noted ΔT remains lower than 5 K in theory when the tested device's thermal emissivity is above 0.5 [28]. For the tested sample's critical case with low thermal emissivity, it is possible to increase this latter by using the Nextel velvet coating 811–21® black paint.

Fig. 3 shows the stability of both the heat power supplied to the measuring cell by the temperature controller and the liquid nitrogen tank (cryotank) versus time. This allows highlighting the disturbances produced during the temperature regulation.

TABLE 2. Characteristics of the radiation calorimetric device

Measurement range	Absolute error	Temperature range	Threshold: Voltage / frequency
15 mW to 10 W	2 mW for 100 mW power loss	-50 °C to 150 °C	3 kV / 1 MHz

One can observe that the cryotank refilling (i.e., each 12 h although its autonomy is 24 h) affects the heat power supplied by the temperature controller of about 30 mW and leads to a temperature change cryotank of about 0.15 °C. Note that the disturbances of the liquid nitrogen refilling on the heat power supplied are cycling with a period of about 12 h. The cryotank refilling leads to additional cooling of the calorimeter and then the measuring cell. The temperature controller reacts to this disturbance by increasing the heat power supply of about 7.5 mW/h for about two hours to maintain the measuring cell temperature setpoint. After this period, the controller heat power supply starts to decrease linearly (5 mW/h slope) during six hours because of the reheating of the cryotank caused by nitrogen evaporation. The decrease phase is followed by a relatively slow increase period (1 mW/h slope during four hours).

Therefore, the nitrogen refilling should lead to an error of about 10 mW (1%) for a heat power loss of 1 W in the controller heat power decrease phase, with a measurement duration of 2 h (worse case). And this error should be about 10% for 100 mW power loss and 33% for 15 mW (1 h measurement duration).

However, the calorimeter's calibration has been carried out regardless of the influence of the measuring cell external current leads because of their thermalization and the low thermal emissivity of the external surface of the cell. The tested component used for the calibration is a wire – wounded resistor of constantan of 1047.2 Ω at 20 °C [27, 29]. The copper current leads inside the measuring cell are 1 mm^2 cross-section and 10 cm in length, and the maximum current supplying the resistor is lower than 50 mA. Therefore the heat losses due to current leads inside the measuring cell are negligible (lower than 10 µW).

As a result, a power loss of 14 mW has been measured with an accuracy better than 12%. This accuracy is better than 2% for heat power losses higher than 100 mW [29]. These measurements are performed exclusively from the decrease phase after the cryotank refilling (2 h after the refilling).

Therefore the calibration of the calorimeter shows an accuracy better than that expected. Note that the quantity P_0 (DUT off) is measured during each cycle of refilling to reduce this latter's influence on measurement accuracy. At the same time, P_1 (DUT on) is measurement just when the measuring cell temperature reached the setpoint again.

However, to limit the influence of the cryotank refilling on the controller heat power supply for better measurement accuracy completely, a continuous filling of the tank is needed. Such a method should need more sophisticated equipment.

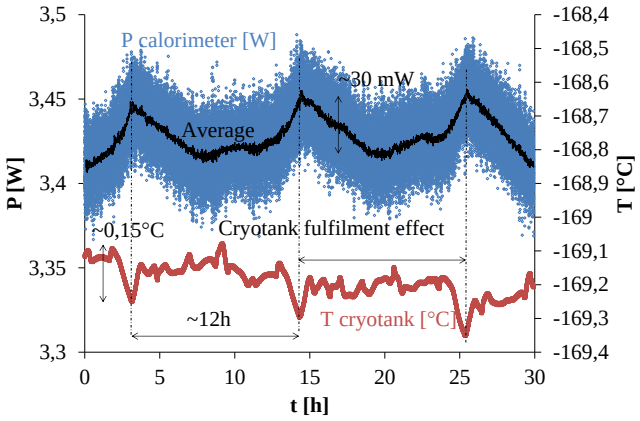

Fig. 3. Change in the heat power supplied by the controller to set the measuring cell at 30 °C and the temperature of this cell versus time and cryotank fulfillment

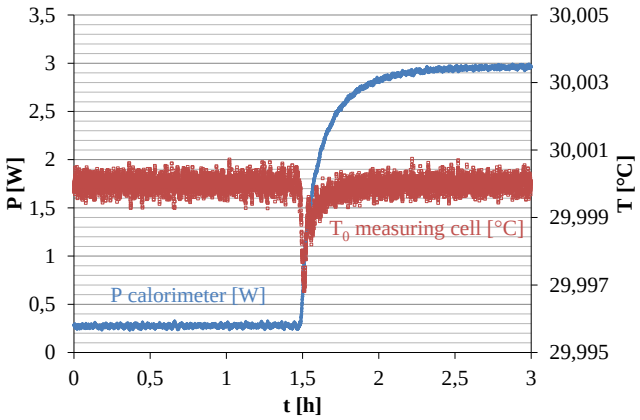

Fig. 4. The time response of the controller heat power supplied to the measuring cell regulated at 30 °C and the temperature of this latter versus time during the change in the status of the DUT from "DUT on" to "DUT off."

Fig 4 gives the change in the heat power supplied by the controller to the measuring cell and the latter's temperature as a function of time just before and after the DUT was switched off. This graph allows us to see the accuracy and response time of the temperature controller. Thus one can

note that a time interval of 2 hours between the "DUT on" and "DUT off" is enough to measure 2.7 W of heat power loss. As observed in Fig 4, the measuring cell temperature controlled by F2 (Fig 2) is within ± 4 10^{-4} °C. Measurements duration being strongly dependent on the dissipated heat power loss increases with the increase of power loss and conversely.

The frequency is an important parameter for various applications; therefore, our calorimeter device has been designed to investigate the DUT with frequency ranging from 0 to 1 MHz. The limitation in frequency here depends only on the current leadership characteristics, which can be adapted to the measurement conditions. Note that the BNC adapter mounted on the measuring cell for the DUT power supply is used up to 5 MHz.

III. PRESENTATION OF TESTED COMPONENTS

We have chosen to study different components that are very well-known in the design of electronic power systems and for their ability to measure losses with different devices under the same experimental conditions.

A. Electrical resistance

Six-wire wounded resistors to make the electrical resistance of 500 Ω (± 1%), 4 W connected in parallel and equivalent to a resistance of 71.6 Ω at ambient temperature (23 °C) and that the copper loss is about 2 W under 12 V, DC applied voltage. The thermal stability of the component is 600/7 ppm/°C (i.e., 4 mΩ for a ΔT = 40 °C).

B. Fly-back converter

The device under test used for power loss estimation is a static converter based on a flyback topology (SW02112 provided by SWITCHY) (Fig. 5.). It is used in strongly thermal constraints environments with an applied A.C. voltage and a frequency ranging respectively from 65 V to 265 V (rms) and 47 to 440 Hz. The converter's D.C. output voltage is 12 V with a rated current of 167 mA when the load resistance is 71.6 Ω.

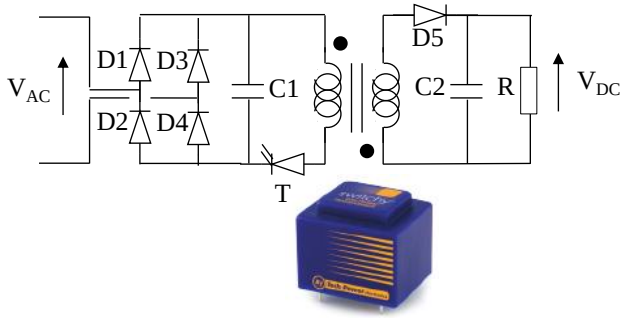

Fig. 5. Schematic diagram (without D.C. voltage controller system) and photography of the SW02112 encapsulated in a resin

C. Self – inductance and capacitor

We investigated distinctly and successively two types of self–inductance and a capacitor, all of them connected in series according to Fig. 6. The power supply is achieved by a half-bridge converter in which the output voltage is 150 V and variable with the frequency. The duty cycle is adjusted to maintain a triangular signal of current as close as possible to 1 A rms.

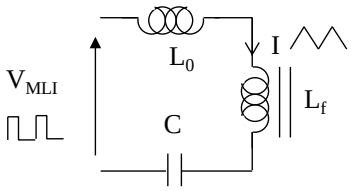

Fig. 6. Schematic diagram used for the investigation of the power loss in toroidal inductance with soft iron core. Power losses measurements by calorimeter is performed on each of these components: L_f = 30 µH, L_0 = 0.5 µH, C = 30 µF, V_{MLI} d. c. = 150 V, I = 1_{RMS} = 1 A.4

The self–inductances are made with 21 whorls of Litz wire (50 strands of 0.355 mm diameter) of 4.95 mm^2 equivalent cross-section. The whorls are coiled around: a toroidal soft iron core of type Magnetics High Flux, 125µ, C058906A2 (Lf = 78 µH) or a dry wood core (L_0 = 0.5 µH). The cores with the same geometric characteristics are made with 221 mm^2 cross-section, 79 mm external diameter, 48 mm internal diameter, and 17 mm height. The wood core allows the measurements of "copper loss exclusively" in inductance for loss separation (Fig. 6).

The capacitor (CDE UNL4W30K–F) is of dry coiled topology (C = 30 µF) based on the metalized polypropylene (P.P.) with low loss (ESR = 6 mΩ at 100 kHz/ 25 °C).

IV. RESULTS AND DISCUSSION

A. Stability and accuracy of measurements versus time and temperature

Fig 7 represents the quantity $P_0 – P_1$ as a function of time measured at different imposed measuring cell temperatures: 20 °C and 40 °C. The component investigated here is the electrical resistance of 71.6 Ω for which the thermal drift between 20 °C and 40 °C is negligible.

One can observe that the calorimeter's power loss is equal to 1.982 W when the measuring cell is set at 40 °C. This power loss is 1.45% lower than what the wattmeter measured. The wattmeter used for our power loss measurement is the Chauvin Arnoux C.A. 405 type with 2.5% and 1% accuracies respectively for D.C. and A.C. Therefore, the result obtained here (Fig 7) is faithful with the accuracy of the calorimeter, the typical error being 2%. For fewer than two hours, it is observed that power loss is almost stable versus temperature with a precision of 0.25%.

Nevertheless, these results allow the estimation of power losses provided by the resistance with a precision of 1.6%.

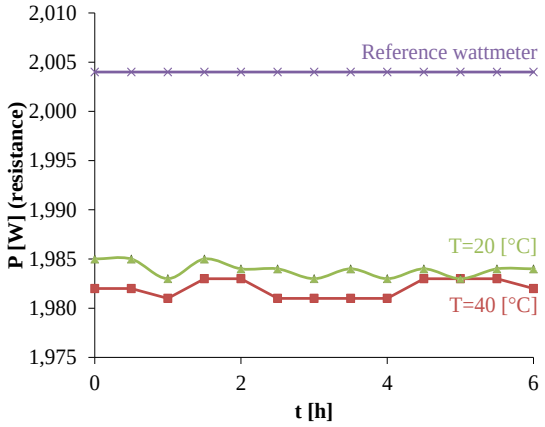

Fig. 7. Power losses $P_0 – P_1$ of equivalent resistance of 71.6 Ω as a function of time at different measuring cell controlled temperature of 20 °C, 40 °C

B. Power loss measurement in flyback SW02112 as the function of A.C. applied voltage

Fig. 8 highlights the behavior of heat power losses ($P_0 – P_1$) of the loaded fly–back converter as a function of the A.C. applied voltage when the measuring cell is set at 30 °C in comparison with the wattmeter measurements.

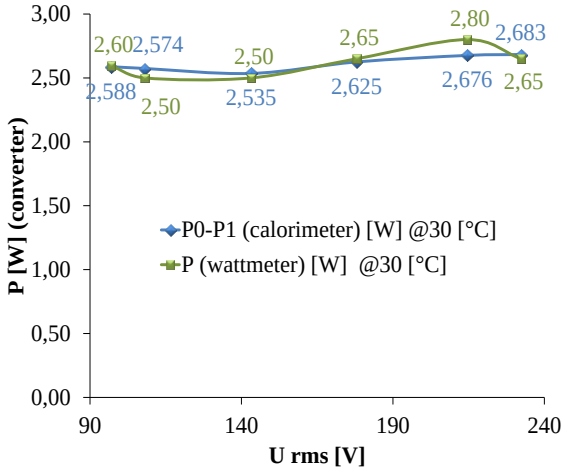

Fig. 8. Change in power loss (P_0–P_1) of the loaded converter as functions of the 50 Hz applied voltage when the measuring cell is controlled at 30 °C in comparison with the power loss measured with a wattmeter (IES ISW8300)

With 230 V_{RMS} applied voltage supplying the converter power losses measured by the calorimeter, it is 2.683 W, while the same measurement performed with the wattmeter has 2.65 W. In general, it is observed that power losses measured by the calorimeter are closed to that measured by the wattmeter, and the difference between these measurements is lower than 0.045 W (5%).

C. Power loss measurements for a self–inductance with a wood core versus frequency

Fig. 9 highlights the change of losses ($P_0 – P_1$) of the self–inductance with a toroidal dry wood core as a function of the applied frequency when the measuring cell is set at 30 °C. Owing to the core material, the heat power loss measured here is exclusively the copper loss.

The heat power losses measured show a stable characteristic for the frequency ranging from 20 kHz to 80 kHz, and any skin effect does not appear on the measurements. All measurements of power losses performed in the present case are 161 mW to 142 mW.

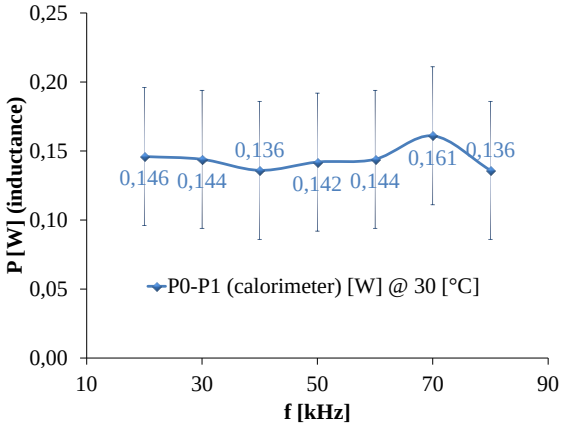

Fig. 9. Power loss measurements ($P_0 – P_1$) in the wood core inductance (L_0 = 0.5 µH) versus applied frequency ranging from 20 kHz to 80 kHz when the measuring cell is controlled at 30 °C (i.e., the temperature of the tested sample ≈ 42 °C)

The cross-section radius of the wire coiled in our self–inductance (0.178 mm) being lower than the skin depth (0.233 mm for 80 kHz in copper at 25 °C); the skin effect is therefore negligible. Losses due to the proximity effect are also insignificant because of the low number of whorls in the coil distributed over a single layer.

The theoretical value of the D.C. resistance of our self–inductance is 10 mΩ. Therefore the expected value of losses should be in the order of 10 mW (Irms = 1 A). The higher quantity of losses measured highlights the importance of connectors and current leads within the calorimeter. Indeed connectors introduce a significant series resistance.

D. Power loss measurements for a self – inductance with a soft iron core versus frequency

Fig. 10 shows the change in power losses ($P_0 – P_1$) of a self–inductance with a toroidal soft iron core, as a function of the applied frequency when the measuring cell is set at 30 °C.

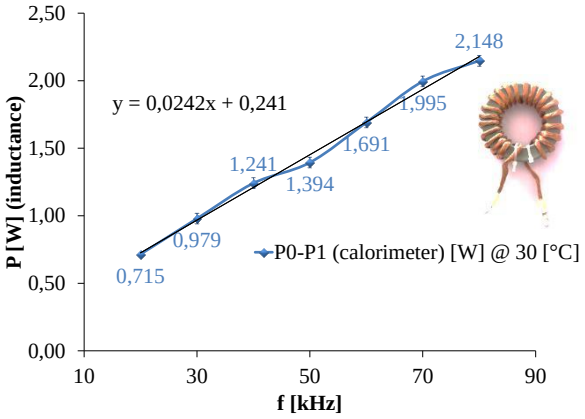

Fig. 10. Fig. 10. Power loss measurements ($P_0 – P_1$) in a self – inductance with a toroidal soft iron core (L_f = 30 µH) versus applied frequency ranging from 20 kHz to 80 kHz when the measuring cell is controlled at 30 °C (i.e., the temperature of the inductance ≈ 50 °C).

One can observe a regular increase in power losses with frequency in all the frequency range. It is noted, therefore, that these losses have tripled from 20 kHz to 80 kHz. They are ranging from 715 mW to 2148 mW.

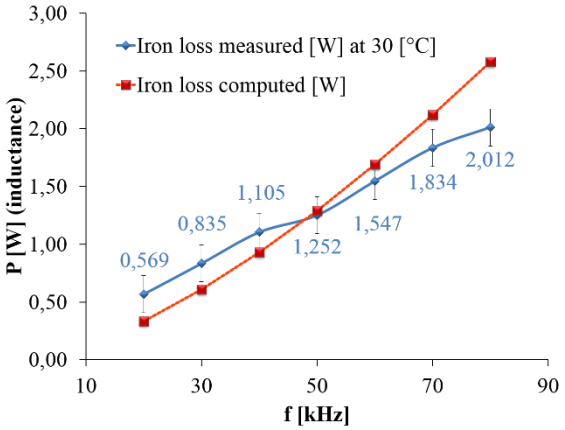

Fig. 11. An estimate of iron losses of our self-inductance with a toroidal soft iron core versus frequency supply ranging from 20 kHz to 80 kHz. The measuring cell was controlled at 30 °C, and Iron losses have been obtained by removing the copper losses (fig. 9) to the global losses (fig 10) and are compared with the predicted losses from the Steinmetz model

The measurements carried out here include iron losses, copper losses due to the self–inductance itself, and the losses produced by the ends of the wire supplies.

Fig. 11 offers an estimate of iron losses obtained by subtracting copper losses (Fig. 9) to the global losses (Fig.10) of the self–inductance. The iron losses of our self–inductance are compared to those estimated from the Steinmetz model [34].

The Steinmetz model gives a good evaluation of the loss level and its change. This model is less realistic when the waveform of electrical signals is far from the sinus shape, which is the case here since the current is triangular and strongly non–symmetric. We cannot compare our measurements to the theoretical results from that model; however, we can see that the level and the change of both cases' losses are consistent.

E. Power loss measurements for a film capacitor versus frequency

Fig. 12 emphasizes the power losses change ($P_0 – P_1$) of a film capacitor versus the applied frequency when the measuring cell is set at 30 °C.

One can observe that the measured losses increase by about 40% from 20 kHz to 80 kHz. These losses are ranging from 174 mW to 244 mW.

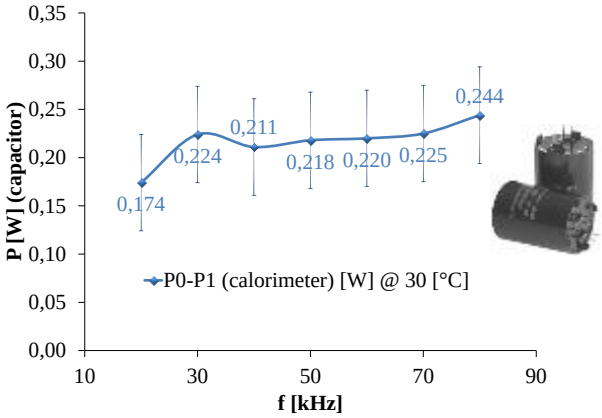

Fig. 12. Power loss measurements (P0 – P1) in a film capacitor (C = 30 µF) versus applied frequency ranging from 20 kHz to 80 kHz when the measuring cell is controlled at 30 °C (i.e., the temperature of the capacitor ≈ 42 °C).

Such capacitors' power losses are renowned decreasing and then increasing versus the frequency (losses in V shape). According to the capacitor's value, dielectric losses level (characterized by the dissipation factor tanδ), and metallic losses (characterized by the square resistance of electrodes: Rsq), the minimum is typically in the range of 10 kHz to 1000 kHz. In the case of capacitors based on P.P., the decrease in power losses is 1/f (where f stands for the frequency) because the tanδ and the permittivity are known as almost stable versus the frequency. The increase of power loss is due to the skin effect for which thickness evolved as a function of f^x (x = ½), leading to the raise of the power losses as a function of f^y (y> ½). Finally, in the capacitors' case, based on the metalized P.P. with low losses, the minimum can behave as a stable state in nearly a decade [35, 36].

It appeared that the frequency range used in this study is too narrow to reveal these two great tendencies, which are the dielectric loss and the metallic loss. We are probably located around the upper of the tendency's tendency frequency since a slight increase in the losses versus the frequency is observed.

Finally, the calorimeter's heat power is gross power loss composed by the component loss and the losses due to the electrical contacts and wires. Therefore, it is desirable to model or measure these losses to extract the component's external contribution and access then to its equivalent series resistance (ESR). Therefore we proceeded to these measurements, and we obtained the power losses due to the electrical contacts and wires ranging from 134 mW to 142 mW between 20 kHz and 80 kHz. By removing these losses to the power losses measured with the film capacitor, the net losses range from 40 mW to 102 mW. The applied current (rms) being set at 1 A, the ESR of the capacitor seen by the calorimeter would be ranging between 40 mΩ and 102 mΩ, which is far greater than the ESR given by the manufacturer (i.e., 6 mΩ at 20 °C and for a frequency of 100 kHz).

The ESR of the capacitor would only represent 4.3 % of the total ESR, which includes the dry ohmic contacts (in a vacuum) and current leads. This low ratio likely makes difficult the fair estimate of the own ESR of the component. This last result put into perspective two subsidiary experiences: (1) evaluate the repeatability of that measure concerning the variability of ohmic contacts; (2) carry out the measure of the total ESR using an impedance bridge circuit in situ (DUT and calorimeter).

V. CONCLUSIONS

The infrared calorimeter designed and implemented has allowed the measurement of power losses of electrical resistance (with 2% accuracy), a fly–back converter, a self–inductance, and a capacitor.

This calorimeter device presents a large operating temperature range (–50 °C to 150 °C). It needs a relatively long preparation time of measurements (48 h) but leads to a relatively short measurement time (2 h). It has been shown that the measurable heat power loss extended from 14 mW to 10 W with great accuracy (2% for heat loss higher than 100 mW).

These measurements also showed the importance of the calibration and the quality of dry contacts to obtain a good measurement accuracy for low values of losses.

These benefits make the I R calorimeter an interesting device for low loss measurement and/or performance evaluation of power components and systems in an isothermal environment for both research and development.

ACKNOWLEDGMENT

The authors wish to thank Service Etudes et Réalisation d'Appareillages Scientifiques (SERAS institut Néel) for technical assistance on the I.R. calorimeter.

REFERENCES

[1] C. Milleret, Convertisseurs d'électronique de puissance et systèmes numériques en aéronautique: application au radar météo, Laboratoire de Génie Electrique de Grenoble (G2Elab – LEG) UMR 5269, Thèse, 2009.

[2] V.Smet, Fiabilité et analyse de défaillances de modules de puissance à IGBT in JCGE'08 Lyon, Décembre 2008.

[3] S. Lefebvre, F. Miserey, Composants à semi-conducteur pour l'électronique de puissance, Tec et Doc, Hermès – Lavoisier, 1er Edition, 2004.

[4] C. Xiao, G. Chen, W. G. H. Odendaal, Overview of Power Loss Measurement Technics in Power Electronics Systems, in Industry Applications, IEEE Transaction on, 43(3) (2007) 657 – 664.

[5] H. Y. Leung, D. M. Budgett, A. Taberner, P. Hu, Power loss measurement of implantable wireless power transfer components using a Peltier device balance calorimeter, IOP Publishing Measurement Science and Technology, 25, Xx-xx August 2014.

[6] G. S. Dimitrakakis, E. C. Tatakis, A. ChNanakos, A Simple Calorimetric Setup for the Accurate Measurement of Losses in Power Electronic Converter, Power Electronics and Applications (EPE 2011), Proceedings of the 2011-14th European Conference on, pp. xx – yy, 30 Aug.-1 Sept. 2011.

[7] P. Hansen, F. Blaabjerg, K. D. Madsen, An accurate power loss measurement method in energy-optimized apparatus and systems, EPE'99-Lausanne.

[8] Yang Liu, Liming Shi and Yaohua Li, Comparison analysis of loss calculation methods and measurement techniques in power electronics and motor systems, in Proc. International Conference on Electrical Machines and Systems (ICEMS), Busan, (2013) 530-534.

[9] V. Loyau, M. LoBue, and F. Mazaleyrat, Comparison of Losses Measurement in a Ferrite With Two Calorimetric Methods, in IEEE Trans. on Magnetics, 46(2) (2010) 529-531.

[10] H. Li., X. Li, Z. Zhang, J. Wang, A Simple Calorimetric Technique for High-Efficiency GaN Inverter Transistor Loss Measurement, Wide Bandgap Power Devices and Applications (WiPDA), 2017 IEEE 5th Workshop on, 251 – 256.

[11] R. Kamei, T.-W. Kim, A. Kawamura, Accurate Calorimetric Power Loss Measurement for Efficient Power Converters, IECON 2011 - 37th Annual Conference on IEEE Industrial Electronics Society, 1173 – 1178,(2011) 7 – 10.

[12] F. Carastro, J. C. Clare, M. J. Bland, P. W. Wheeler Calorimetric Loss Measurements and Optimization of High Power Resonant Converters Pulsed Applications, Power Electronics and Applications, 2009. EPE '09. 13th European Conference on, (2009) 8-10.

[13] P. D. Malliband, N. P. van der Duijn Schouten, R. A. McMahon, Precision Calorimetry for the Accurate Measurement of Inverter Losses," Power Electronics and Drive Systems,. PEDS. The Fifth International Conference on, 321 – 326, (2003) 17-20.

[14] S. Weier, M. A. Shafi, R. McMahon, Precision Calorimetry for the Accurate Measurement of Losses in Power Electronic Devices, IEEE Transactions Industry Applications, 46(1) (2010) 278 - 284.

[15] D. Christen, U. Badstuebner, J. Biela, J.W. Kolar, Calorimetric Power Loss Measurement for Highly Efficient Converters, The 2010 International Power Electronics Conference, 1438 – 1445.

[16] E. Ritchie, J. K. Pederson, F. Blaabjerg, P. Hansen, Calorimetric measuring system, in Industry Applications Magazine, IEEE, 10 (3), (2004) 70–78.

[17] C. Buttay, Contribution à la conception par la simulation en électronique de puissance, application en l'onduleur basse tension ,

Thesis of Institut National des Sciences Appliquées de Lyon, 92-97 (2004).

[18] D. R. Turner, K. J. Binns, B. N. Shamsadeen, D. F. Warne, Accurate measurement of induction motor losses using balance calorimeter, Proc. IEEE, 138(5) (1991) 680-685.

[19] A. Jalilian, V. J. Gosbell, B. S. P. Perea, P. Cooper, Double chamber calorimeter (DCC): a new approach to measure induction motor harmonic losses, IEEE Transactions on Energy Conversion, 14(3) (1999) 680-685.

[20] P. Rasilo, J. Ekström, A. Haavisto, A. Belahcen, A. Arkkio, Calorimetric System to measure synchronous machine losses, IET Electric Power Applications, 6(5) (2012) 286-294.

[21] F. Zámborszky, D. Tóth, Z. Palánki, E. Csizmadia, Electrical and Calorimetric Power Loss Measurements of Practically Ideal Soft Magnetic Cores, IEEE Transaction on Magnetics, 50(4) 2014.

[22] J. K. Bowman, R. F. Cascio, M. P. Sayani, T. G. Wilson, A Calorimetric Method for Measurement of Total Loss in Power Transformer, Power Electronics Specialists Conference, 1991. PESC '91 Record, 22nd Annual IEEE, 24-27 (1991) 633 – 640.

[23] D. Rothmund, D. Bortis, and J. W. Kolar, Accurate transient calorimetric measurement of soft-switching losses of 10kV SiC MOSFETs, in Proc. IEEE International Symposium on Power Electronics for Distributed Generation Systems (PEDG), Vancouver, BC, (2016) 1-10.

[24] B. Seguin, J. P. Gosse, Dispositif de mesure calorimétrique des pertes dans les condensateurs de puissance, Journal de Physique III France, (1997) 321-336.

[25] E. Obame, O. Gallot-Lavallée, F. Aitken, Review and improvement of a method for measuring losses in the dielectric materials by calorimetry, International Conference on Broadband Dielectric Spectroscopy and its Applications (BDS) Lyon, France, 2008.

[26] G. Chen, C. Xiao, W. G. Odendaal, An apparatus for loss measurement of integrated power electronics module: design and analysis, Industry Applications Conference. 37th IAS Annual Meeting. Conference Record of (1) (2002) 222- 226.

[27] E. Obame, O. Gallot-Lavallée and F. Aitken, Développement d'un dispositif de calorimétrie par rayonnement thermique : application à la mesure des pertes dans les composants électriques, Thesis of Institut Polytechnique de Grenoble, (2010) 16-24.

[28] E. ObameNdong, O. Gallot – Lavallée, F. Aitken, Analytical heat transfer modeling of a new radiation calorimeter, in ThermochemicaActa 633 (2016) 56 – 68.

[29] O. Gallot – Lavallée, F. Aitken, E. ObameNdong, « Système calorimétrique et procédé pour mesurer les pertes de puissance dans un composant électrique », N° Brevet FR2962539, N° Enregistrement 1055474, Paris, France, Enregistré le 06 – 07 – 2010, Publié le (2012) 13 – 01.

[30] N. J. Simon, E. S. Drexler, R. P. Reed NIST monograph 177 properties of copper and copper alloys at cryogenic temperature, (1992) 7-23.

[31] E. Tang – Kwor, S. Mattei Emissivity measurements for Nextel velvet coating 811 – 21 between – 36 °C to and 82 °C, High Temperatures, High pressures, 33(5) (2001) 551 – 556.

[32] S. Ogarev, M. Samoylov, V. Sapritsky, A. Panfilov, of Thermophysics, 30 (2009) 77-97.

[33] JUMO Régulation S. A. Eléments sensibles en platine sous céramique suivant EN 60 751, Fiche technique 90.6022, Janvier 2009.

[34] Jieli Li, Abdallah T, Sullivan C.R., Improved calculation of core loss with nonsinusoidal waveforms, IEEE Industry Applications Conference Record, 4 (2001) 2203-2210.

[35] B. Seguin, « les pertes dans les condensateurs bobinés utilisés en électronique de puissance : mesure calorimétrique et modélisation », Thèse dirigée par Jean – Paul Ferrieux et Jean – Paul Gauss, Institut National Polytechnique de Grenoble, (1997) 1 – 198.

[36] R. E. Lafferty, Capacitor loss at radio frequencies, IEEE Transactions on Components, Hybrids and Manufacturing Technology, 15(4) (1992) 590 – 3.

[37] Ajay Kumar Lal Control Actions Measurement to Propagation of Cascading Outages in the Power System, International Journal of Engineering Trends and Technology (IJETT), 53(1) (2017)1-6 November. ISSN:2231-5381. www.ijettjournal.org